Control of the Interchain π−π Interaction and Electron Density Distribution at the Surface of Conjugated Poly(3-hexylthiophene) Thin Films

ARTICLE *in* THE JOURNAL OF PHYSICAL CHEMISTRY B · OCTOBER 2007

Impact Factor: 3.3 · DOI: 10.1021/jp0732209 · Source: PubMed

7 AUTHORS, INCLUDING:

Xiao-Tao Hao
Shandong University
69 PUBLICATIONS **1,293** CITATIONS
SEE PROFILE

Takuya Hosokai
Iwate University
40 PUBLICATIONS **357** CITATIONS
SEE PROFILE

Satoshi Kera
Institute for Molecular Science
144 PUBLICATIONS **2,595** CITATIONS
SEE PROFILE

Nobuo Ueno
Chiba University
333 PUBLICATIONS **5,377** CITATIONS
SEE PROFILE

Control of the Interchain $\pi-\pi$ Interaction and Electron Density Distribution at the Surface of Conjugated Poly(3-hexylthiophene) Thin Films

X. T. Hao,*,† T. Hosokai,‡ N. Mitsuo,‡ S. Kera,†,‡ K. K. Okudaira,†,‡ K. Mase,§ and N. Ueno†,‡

Faculty of Engineering, Chiba University, Chiba 2638522, Japan, Graduate School of Science and Technology, Chiba University, Chiba 2638522, Japan, and Institute of Materials Structure Science, Tsukuba, Ibaraki, 3050801, Japan

Received: April 26, 2007; In Final Form: June 27, 2007

Interchain interaction, i.e., $\pi-\pi$ stacking, can benefit the carrier transport in conjugated regio-regular poly(3-hexylthiophene) (P3HT) thin films. However, the existence of the insulating side hexyl chains in the surface region may be detrimental to the charge transfer between the polymer backbone and overlayer molecules. The control of the molecular orientation in the surface region is expected to alter the distribution of the π electron density at the surface to solve such problems, which can be achieved by controlling the solvent removal rate during solidification. The evidence that the π-electron density distribution at the outermost surface can be controlled is demonstrated by the investigation using the powerful combination of near edge X-ray absorption fine structure spectroscopy, ultraviolet photoelectron spectroscopy, and the most surface-sensitive technique: Penning ionization electron spectroscopy. From the spectroscopic studies, it can be deduced that the slower removal rate of the solvent makes the polymer chains even at the surface have sufficient time to adopt a more nearly equilibrium structure with edge-on conformation. Thus, the side hexyl chains extend outside the surface, which buries the π-electron density contributed from the polymer backbone. Contrarily, the quench of obtaining a thermo-equilibrium structure in the surface region due to the faster removal of the solvent residual can lead to the surface chain conformation without persisting to the strong bulk orientation preference. Therefore, the face-on conformation of the polymer chain at the surface of thin films coated with high spin coating speed facilitate the electron density of the polymer backbone exposed outside the surface. Finally, thickness dependence of the surface electronic structure of P3HT thin films is also discussed.

1. Introduction

The structure−property relationship of solution−processible conducting polymers with π-conjugated electronic structures have been explored extensively due to their significant impact in optoelectronic applications[1−3] such as polymer light emitting diodes, field effect transistors and polymer solar cells, etc. Polythiophene and its derivatives are the first conducting polymers that are stable toward oxygen and moisture. The unsubstituted conjugated polythiophene (PT) has relatively stiff chains with little flexibility due to the strong interchain $\pi-\pi$ interaction that makes them insoluble and nonprocessible. A family of poly(alkylthiophenes) has been synthesized to make soluble and processible conducting polythiophenes with preserved π electronic structure.[4] Solution-processed regioregular conjugated poly(3-hexylthiophene) (P3HT) thin films can easily lead to well-organized conformation leading to highly oriented polymer films, and such films in general have complex microstructures with ordered microcrystalline domains embedded in an amorphous matrix.[2,5]

Due to its unique characteristics with rigid backbone and solubilizing flexible side chains, P3HT usually serves as a prototypical semiconducting polymer to be employed in the application and properties characterization. The long-range order and $\pi-\pi$ interchain stacking in the P3HT thin films play an important role on the charge transport process and the device performance, which have been characterized comprehensively.[2,6−12] The structural characteristics are therefore well understood in the bulk and thin films, but few studies were reported focusing on the details of the surface layers. Delongchamp et al.[13] has pointed out that molecular orientation and hole mobility of P3HT thin films can be varied by spin-coating speed. Molecular orientation is investigated by near edge X-ray absorption fine structure spectroscopy (NEXAFS). The bulk behavior, however, does not necessarily extend to the surface due to the different solvent removal process between the bulk and surface.[14] Therefore, it is essential to determine the conformation and stacking at surfaces, especially at the outermost surfaces that are most adjacent to the overlayer molecules, because the spatial electron-density distribution at these regions might be inconsistent with the bulk region due to the different chain conformation resulting from variation of coating process, and furthermore, it is of particular significance to understand the charge-transfer mechanism with an overlayer molecule due to the $\pi-\pi$ electron wavefunction overlap.

More recently, Ho et al.[15] reported that the chain orientation and $\pi-\pi$ interaction between chain segments at surfaces varied strongly with the deposition solvents indicated by their NEXAFS spectra. However, the commonly used surface spectroscopic tools like NEXAFS, X-ray photoelectron spectroscopy and ultraviolet photoelectron spectroscopy (UPS) do not have required surface sensitivity to detect the electron states tailing

* Author to whom correspondence should be addressed. E-mail: dr.xthao@gmail.com. Present address: School of Chemistry, the University of Melbourne, Australia.

† Faculty of Engineering, Chiba University.

‡ Graduate School of Science and Technology, Chiba University.

§ Institute of Materials Structure Science.

10.1021/jp0732209 CCC: $37.00
Published on Web 08/14/2007

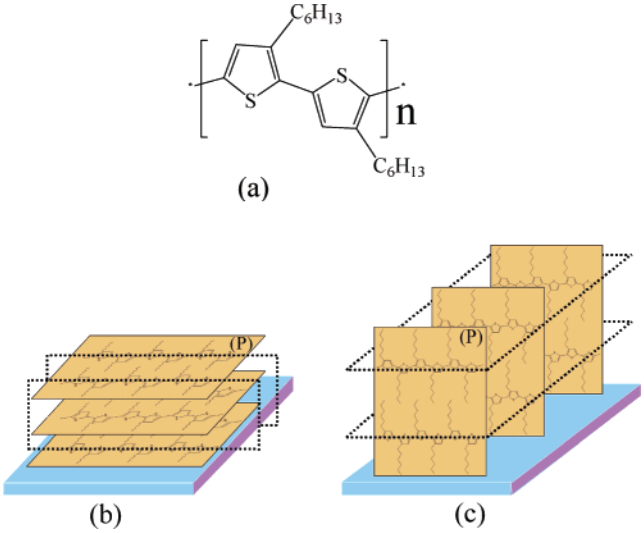

Figure 1. (a) Chemical structure of P3HT. (b) Diagrams of P3HT thin films conformation: (b) face-on and (c) edge-on. Thiophene-ring planes are parallel to the planes (P) shown in (b) and (c); the dashed planes perpendicular to planes (P) correspond to those for lamellar structure.

outside the polymer surface. The spectroscopic tools using X-ray based photons as probes can detect the electronic structures about top ~2 nm or even thicker layer inside the polymer surface and that using ultraviolet photons as probes like UPS can observe the electronic density distribution about top ~1 nm inside the surface. Contrarily, Penning ionization electron spectroscopy (PIES) using metastable atoms (He*) as probes,[16] can observe the outermost surface electrons selectively because metastable atoms do not penetrate into the bulk of the solid and are easily deexcited by overlapping electron wavefunctions of He* and target surface.[17,18] Unlike the ordinary surface sensitive spectroscopic techniques using photons or electrons, PIES can thus be adopted for probing the electronic states exposed outside the polymer surface to understand the chain conformation and spatial distribution of π-electron density at outermost surface.

In this work, we employed a powerful combination of NEXAFS, UPS, and PIES with different surface sensitivities to investigate the surface electronic structure of P3HT (chemical structure shown in Figure 1a) thin films coated with various coating parameters/methods. There is clear evidence showing that the chain conformation and therefore the spatial distribution of the electron density at surface and outermost surface can be controlled by employing different coating parameters/methods. The schematic diagrams of P3HT thin film conformation are also given in Figure 1: face-on (b) and edge-on (c) conformation. In addition, the surface electronic structure of conjugated polythiophene without side chains was also investigated as a reference aiming to understand the conservation of the π electronic structures after attaching the side hexyl-chains.

2. Experimental Section

The P3HT and PT were purchased from Aldrich and used without further purification. The polymer thin films were prepared on gold (100 nm thick)-coated Si (100) wafers by spin casting and dip casting (for P3HT) or vacuum evaporation (for PT). P3HT powder was dissolved into chloroform and the spin casting was performed 60 s with speeds of 3000 and 400 rpm for solution concentrations of 2.5 and 0.5 mg/mL, respectively. The dip casting was very simple by dipping the substrate into the solution (0.5 mg/mL) for 60 s, and then the sample was dried slowly in a chloroform-vapor environment. The thickness (measured by Surfcorder ET-4000A, Kosaka Laboratory Ltd.) is about 5−10 nm controlled by the solution concentration and spin coating process or evaporating parameters, which is thick enough to cover the substrates and thin enough to minimize the charging artifacts during UPS and PIES measurements. Furthermore, P3HT thin films were spin coated with various solution concentrations (from 0.7 to 5 mg/mL) at a fixed spin speed (3000 rpm) to verify the thickness dependence on the surface electronic structure. The spin-coated and dip-coated thin films were then loaded into the UHV chamber immediately and kept for several hours to remove the solvent residual before measurements, and the evaporated film prepared in the preparation chamber was transferred into the analysis chamber for in situ measurement. The solution-processed films were annealed at 453 K under UHV for 1 h to further remove the contamination/solvent and improve the crystallinity. The contamination-free surfaces of the samples can be obtained by the careful preparation in air and a specific loading system with a dry pump as shown in previous works.[18−21] The P3HT samples used in this paper are annealed films unless otherwise specified. It also should be noted that no charging effect is observed for all the thin films except for the specified thicker films.

The synchrotron based NEXAFS experiments were carried out with the total electron yield detection at the beamline 13C at Photon Factory, Institute of Materials Structure Science, Japan. NEXAFS spectroscopy measures the soft X-ray excitation of C1s electrons to unfilled molecular levels. UPS were measured using the He I (21.22 eV) resonance line produced by a dc discharge lamp. In PIES measurements, helium atoms were excited to the metastable states, 2^1S (20.62 eV) and 2^3S (19.82 eV) by a dc discharge. To obtain pure He* (2^3S) atoms, the He* (2^1S) was quenched by a separated dc helium lamp.[17] The spectra were normalized with total electron emission current.

To assign the features of the HOMO and near HOMO regions in the experimental data, hybrid density functional theory (DFT) MO calculation was carried out for model molecules of P3HT (3HT with ten repeated units) and PT (twelve-thiophene) by employing the Becke's three-parameter exchange function[22] combined with the Lee, Yang, and Parr's correlation function (B3LYP).[23] Molecular geometry optimization was done at the B3LYP level using 6-31G* basis set.

3. Results and Discussion

3.1. X-ray Diffraction Patterns of P3HT Thin Films. Solution-processed conjugated P3HT thin films have complex microstructures with ordered microcrystalline domains embedded in an amorphous matrix.[2,5] The X-ray diffraction (XRD) spectra shown in Figure 2a indicate the detected peak at $2\theta = 5.4°$ originates from (100) reflection of P3HT-crystallites with *a*-axis orientation. The (100) reflection and its higher order reflections shown in the diffraction profile correspond to the main chain separation ($d_{100} = 1.60$ nm) in different lamella (shown in inset of Figure 2). Note that the lamellar plane is perpendicular to thiophene ring plane. The parallel order of thiophene-ring planes in P3HT films leads to the high intralamellar mobility in P3HT due to the delocalization of the charge carrier among polymer chains.[24] The annealing effect was very clear to improve crystallinity of the P3HT thin films because the higher order peaks appear and the full width at half-maximum (fwhm) of the diffraction peaks becomes smaller. The fwhm values of the (100) peak before annealing are 1.4°, 1.2°,

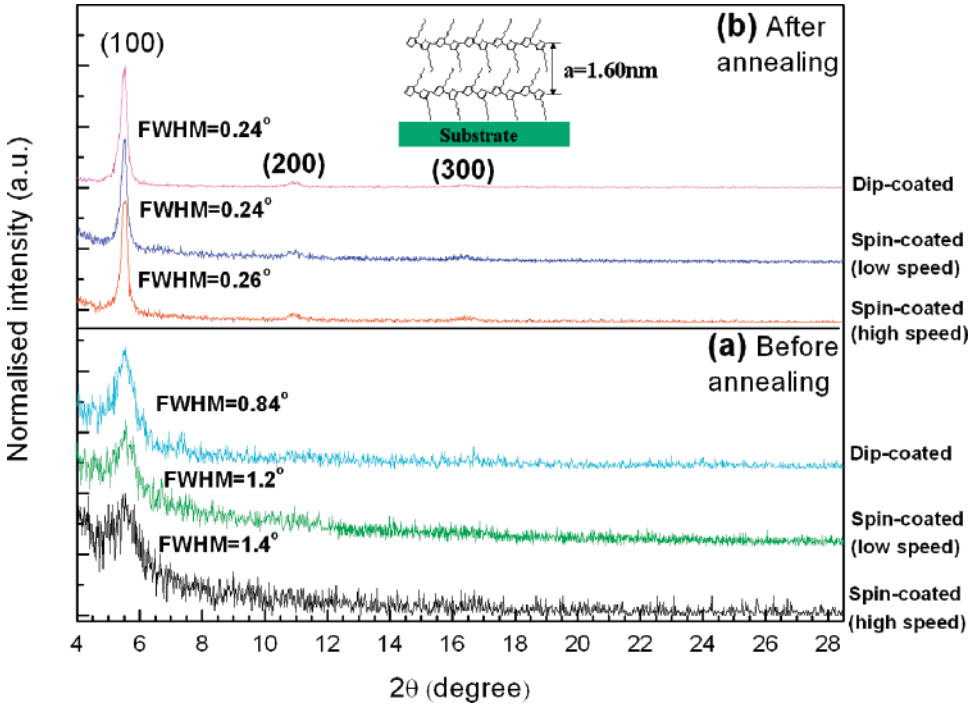

Figure 2. X-ray diffraction spectra of P3HT thin films. (a) Before annealing: sample spin-coated with high speed (bottom curve); sample spin-coated with low speed (medium curve); dip coated sample (upper curve). (b) After 453 K annealing: sample spin-coated with high speed (bottom curve); sample spin-coated with low speed (medium curve); dip coated sample (upper curve). Inset: lamellar structure of P3HT thin film.

and 0.84° for high spin speed, low spin speed, and dip-coated sample, respectively. The smallest fwhm value of the dip-coated sample is due to the slower solvent removal rates in the dip-coating process, which results in the film structure closer to the equilibrium structure with higher crystallinity. After annealing, the fwhm values for all thin films are very similar in the range 0.24−0.26°, indicating that all these thin films may have increased crystalline domains and similar crystallinity levels due to annealing. Not much difference can be observed in the XRD spectra for thin films coated with different methods because of the relatively poor surface sensitivity of this technique.

3.2. NEXAFS Spectra of P3HT Thin Films. Synchrotron-based NEXAFS experiments were carried out on P3HT thin films to quantify the structural difference among the samples coated with different parameters and the spectra are shown in the Figure 3a. The sharp transition resonance situated at 285.3 eV originates from transitions to C=C π^*. The transition peaks situated at 287.8 eV originate from transitions to the superimposed C−H/C−S σ^* orbitals, whereas the broader peak located at 292.9 eV may be associated to transitions to C−C σ^* orbitals. The peak due to the C=C π^* state exhibits a strong systematic variation with the incident angle (θ) (as depicted in Figure 3b) that can determine the average conjugated plane orientation. Calculated results for the π^* intensity as a function of the incident angle (θ) are also shown in Figure 3b using the computation procedure as reported previously.[18,25] For vector-type orbitals, the absolute angle-integrated intensity I_v is given as

$$I_v = A[PI_v^{\parallel} + (1-P)I_v^{\perp}] \quad (1)$$

where A is a constant and P is the degree of photon polarization, taken as 0.9 in this measurement. $I_v^{\parallel}$ and $I_v^{\perp}$ stand for the resonance intensities of the vector orbitals for the parallel and perpendicular components of the electric-field vector. After integrating the azimuthal orientation of the molecule with respect to the substrate normal from 0 to 2π, eq 1 can be expressed as

$$I_v = A\{P[2\pi \sin^2\theta \cos^2\alpha + \pi \cos^2\theta \sin^2\alpha] + (1-P)\pi \sin^2\alpha\} \quad (2)$$

where the incident angle (θ) and molecular tilt angle (α) are defined as shown in the insets of Figure 2. Comparing the experimental π^* intensities with the computed results, the average molecular orientation of polymer backbone can be estimated. The average tilt angle (α) of the plane of polymer backbone with respect to the substrate surface is 62°, 72°, and 70° for samples spin-coated with high spin speed, low spin speed and dip-coated, respectively, which match with the computed curves very well. Therefore, although all the samples have a tilted conformation, dip-coated and low-speed spin-coated samples have greater edge-on characters than the high-speed spin-coated sample, whereas the high-speed spin-coated sample has more face-on characters. The schematic diagrams of face-on and edge-on conformations are shown in Figure 1b,c. The slower solvent removal rate that results in materials closer to their equilibrium structure should be responsible for the edge-on conformation in dip-coated and low-speed spin-coated sample.[13]

In addition, the average tilt angles of the P3HT thin films coated at high spin speed (3000 rpm) with various solution concentrations (0.7, 2.5, and 5 mg/mL) are compared before and after annealing as shown in Table 1. It can be seen that the average tilt angles are in the ranges 55−58° and 59−62° for the thin films before and after annealing, respectively. The chain orientation does not change too much for the different solution concentration at fixed spin speed, but annealed thin films give larger tilt angles showing more equilibrium edge-on conformation.

3.3. Surface Electronic Structure of PT Thin Films. To understand π electronic states contributed from the polymer

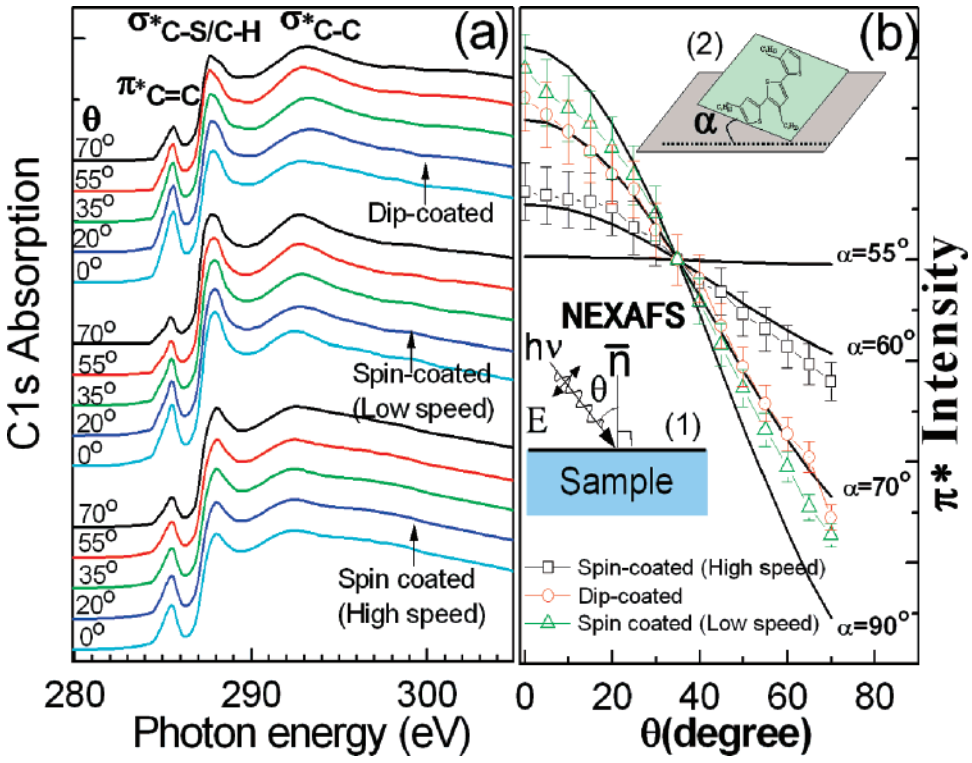

Figure 3. (a) Normalized C K-edge NEXAFS spectra as function of incident X-ray angle of annealed P3HT thin films. (b) C═C π^* intensity variation as a function of the incident angle (θ). Computed curves are labeled with different tilt angles α. Experimental data: (□) high-speed spin-coated sample; (△) low-speed spin-coated sample; (○) dip-coated samples. Insets: (1) gives the measurement geometry of NEXAFS and (2) shows the definition of the tilte angle α of the polymer backbone.

TABLE 1: Summary of the Average Tilt Angles (α, deg) of the P3HT Thin Films Coated with Various Coating Parameters

	n = 5 mg/mL, v = 3000 rpm[a]	n = 2.5 mg/mL, v = 3000 rpm[a]	n = 0.7 mg/mL, v = 3000 rpm[a]	n = 0.5 mg/mL, v = 400 rpm[b]	n = 0.5 mg/mL, dip-coated[c]
α (before annealing)	55	58	55		
α (after annealing)	60	62	59	72	70

[a] Coated at various solution concentrations (n) (0.7, 2.5, and 5 mg/mL) at a fixed spin speed (v) of 3000 rpm before and after annealing. [b] Coated at solution concentration (n) of 0.5 mg/mL at a spin speed (v) of 400 rpm after annealing. [c] Dip-coated at a solution concentration (n) of 0.5 mg/mL after annealing.

backbone, theoretical calculations of the electronic structure of PT were performed and the surface electronic structure of evaporated PT without side chains was investigated by UPS and PIES, as shown in Figure 4. Because there is no effect brought by side pendant groups on the electronic states of PT, the observed features appeared on the spectra are definitely from the polymer backbone. Figure 4 gives the π-electronic states spectral region of (1) UPS spectra (upper curve), (2) PIES spectra (medium curve) for thin films of PT, and (3) calculated density of valence states (bottom curve, calculated for twelve repeated thiophene ring units). Due to many molecular orbitals in close vicinity to each other in the polymer chains as well as solid-state broadening and vibration coupling of the photoemission features,[26,27] the individual molecular orbital cannot be resolved in the spectra, and therefore several molecular orbitals usually contribute to a single photoemission feature in the measured spectra. Although the theoretical calculations usually do not necessarily match with the experimental observations, the observed features of π electronic states can be assigned with the help of the calculations in the low binding energy region from 0 to 5 eV. The features located around ~0.5 to ~1 eV may be assigned to the strongly delocalized, all-C $2p_z$ derived π electronic states, and the features appearing at ~1−2.5 eV should be contributed mainly from π states of C $2p_z$ atomic orbitals (AOs) and partly from the S $3p_z$ AOs. In addition, the peaks located around ~4 eV in UPS and PIES may include localized π states with strong S $3p_z$ contribution and weak contribution of the C $2p_z$ AOs. Because PIES is more surface-sensitive than UPS, the peak position difference in the spectra between UPS and PIES may be due to the difference of AOs distribution, C $2p_z$ and S $3p_z$, at the outermost surface. Usually, S $3p_z$ AOs spread more widely than C $2p_z$ AOs and give more contribution to the electronic wave function distributed at the outermost surface, which can interact more easily with the He* metastable atoms in PIES. Therefore, the peak in PIES that is located at a relatively higher binding energy position (~4.1 eV) than that in UPS (~3.8 eV) should come from π states with more contribution from S $3p_z$ AOs, and the peak in UPS should include more contribution from π states of C $2p_z$ AOs.

3.4. Surface Electronic Structure of P3HT Thin Films. Surface electronic structures of spin-coated and dip-coated P3HT thin films have also been observed by UPS and PIES. As mentioned above, the UPS spectral intensity comes from the top ~1 nm layer inside the thin films (roughly about one or two monolayer of P3HT depending on the conformation), whereas the PIES can only probe the electronic states exposed outside the polymer surface. Therefore, by comparing with the NEXAFS that has much deeper probing depth, we can get the clear picture of π electronic states distribution from inside to outside. Overlap of π electronic wavefunction within the lamellae planes should be responsible for the high intralayer mobility in P3HT films. On the other hand, π electronic states

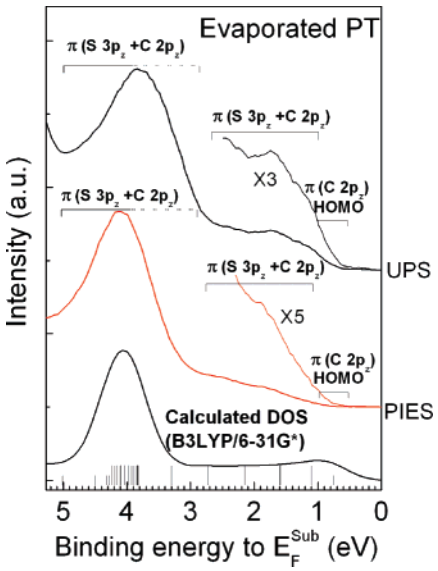

Figure 4. (1) UPS spectra (upper curve), (2) PIES spectra (medium curve) for thin film of PT without annealing, and (3) calculated density of valence states (bottom curve (calculated by a DFT method with the B3LYP/6-31G* basis set on PT with twelve repeated thiophene ring units; the longer bars indicating that the electronic states include the contribution from S3p$_z$ atomic orbitals). The binding energy was measured from the Fermi level of the substrate (E_F^{Sub}).

distributed outside the polymer surface provide the possibility of forming overlap with the π electronic wavefunction of an overlayer molecular material, consequently achieving efficient charge transfer in the related hetero-junction structure used for polymer devices.

Figure 5 gives the UPS spectra for (a) annealed dip-coated, (b) annealed low-speed spin-coated, (c) annealed high-speed spin-coated, and (d) nonannealed high-speed spin-coated P3HT thin films and (e) calculated density of valence states (calculated for ten repeated thiophene ring units). The left panel shows the spectra of the complete valence region, and the right one shows the HOMO spectral region. The binding energy was measured from the Fermi level of the substrate (E_F^{Sub}). The observed features in the spectra can be assigned correspondingly by the calculated results. The stronger peak located at about 3 $\sim$ 4 eV corresponds to the localized π states contributed from S 3p$_z$ and C 2p$_z$ AOs. The observed π states whose feature located around $\sim$0.5$-$1 eV in UPS spectra are due to the strongly delocalized nature of HOMO state of C 2p$_z$ AOs, and the feature around $\sim$1 to $\sim$2.5 eV comes from contribution of C 2p$_z$ and partly contribution of S 3p$_z$ AOs. No clear discernible features appear for all the samples between 5 and 12 eV, which are related to the σ states from the main chain and the hexyl side groups due to the complexity of the polymer structure. The spectra are consistent with the reported UPS results in the literature[7,12] and are comparable to the theoretical calculation in the low binding energy region from 0 to 5 eV. Also, comparing the UPS spectra of PT in Figure 4 and P3HT thin film in the low binding energy (0$-$5 eV), the π electronic structure is found to be conserved approximately after attaching the side hexyl chain onto the polymer backbone. In addition, by comparing spectra c and d of the high-speed spin-coated thin films, the observed electronic structure does not change much except for the stronger intensity for the annealed thin films due to the improved crystallinity and ordered structure after annealing.[18]

As aforementioned in the NEXAFS results, the high-speed spin-coated sample has more face-on characters and low-speed spin-coated and dip-coated samples have more edge-on characters. The different conformation should be responsible for the difference in the UPS spectra of different samples. It can be seen clearly, from Figure 5, that the intensity of peaks related to π states is stronger in the spectrum for the high-speed spin-coated sample than that for low-speed spin-coated and dip-coated samples. This suggests that π electronic wave function is exposed more outside the surface for the sample with face-on conformation and can be detected with less influence of the side chains, and correspondingly generate more photoelectrons for higher spectral intensity. For the high-speed spin-coating process, there is too little time to achieve equilibrium structure in the thin film due to rapid evaporation of the solvent and therefore the polymer chains at surface regions may be assembled with more face-on conformation before any significant crystallization or molecular orientation reorganization occurs.[13] However, the π states are shielded more by the side chains for the samples with edge-on conformation. Although the probing depth allows UPS to detect the electronic states of the polymer backbone, the corresponding intensity in the UPS spectra becomes weaker due to the shielding by side chains. On the basis of this assumption, we may conclude that the dip-coated sample most likely has more edge-on confirmation than the low-speed spin-coated sample in the top one or two monolayers near the surface because the intensity of peaks related to the π states is much weaker in the spectrum for the dip-coated sample than that for low-speed spin-coated sample. This should be due to the slower solvent removal rate of dip-coated sample at not only the bulk region but also the surface region, which enables the polymer chain to have sufficient time for achieving the equilibrium edge-on conformation.[13]

Considering that the PIES has much greater surface sensitivity, it is adopted to prove the viewpoint mentioned in the UPS results. PIES spectra for (a) annealed dip-coated P3HT thin films, (b) annealed low-speed spin-coated, (c) annealed high-speed spin-coated, and (d) nonannealed high-speed spin-coated P3HT thin films are given in Figure 6. The left panel shows the spectra of the complete valence region, and the right one shows the HOMO spectral region. The binding energy was measured from the Fermi level of the substrate (E_F^{Sub}). For high-speed spin-coated sample, the π states ($\sim$1 to $\sim$2.5 eV and $\sim$3 to $\sim$4 eV) contributed by C 2p$_z$ and S 3p$_z$ AOs are shown clearly in the spectra, indicating that the π electronic wave function from the polymer backbone is distributed outside the polymer surface for the high-speed spin-coated sample and can effectively interact with metastable atoms He*. Correspondingly, the HOMO molecular orbital from the polymer backbone also can be detected by He* metastable atoms showing a clear feature in the range of the binding energy of $\sim$0.5 to $\sim$1 eV, which is believed to be facing the vacuum at the polymer surface. However, there are less obvious features for low-speed spin-coated and dip-coated samples in the π states region (0$-$4 eV), indicating that the electronic states from the polymer backbone are more shielded by the side alkyl chain than the high-speed sample and cannot interact with the metastable atoms. The very weak shoulders around $\sim$3$-$4 eV in the spectra of both low-speed spin-coated and dip-coated samples and that around $\sim$1$-$2.5 eV in the spectra of low-speed spin-coated thin film can be observed because of the wider spreading nature of S 3p$_z$ AO. Due to the great surface sensitivity of PIES, we believe that high-speed spin-coated samples adopt more face-on orientation in the surface region different from the tilted conformation inside the film, whereas the low-speed spin-coated and dip-coated samples adopt tilted or more edge-on conforma-

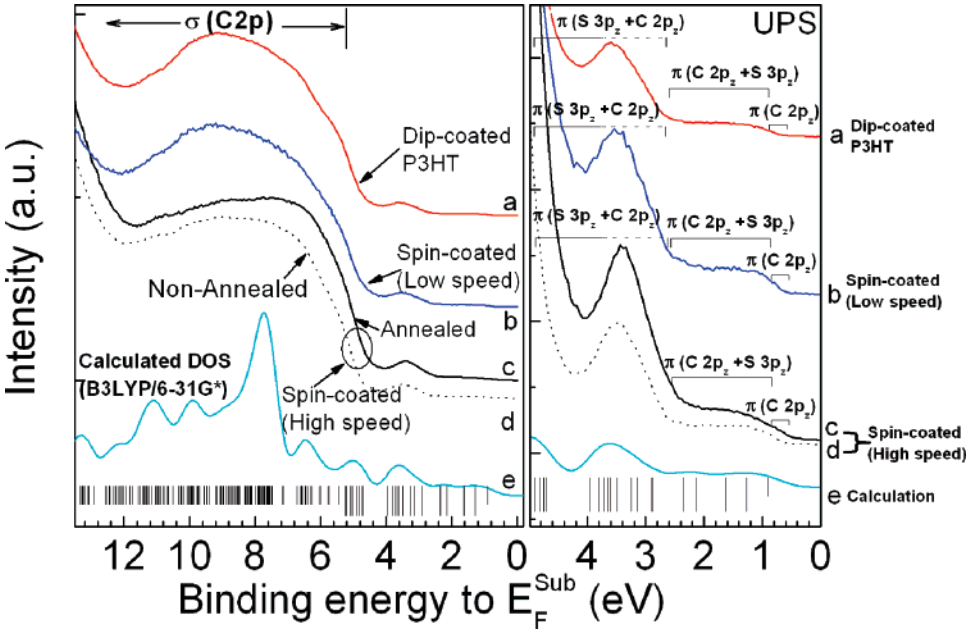

Figure 5. UPS spectra for (a) annealed dip-coated P3HT thin films, (b) annealed low-speed spin-coated, (c) annealed high-speed spin-coated, and (d) nonannealed high-speed spin-coated and (e) calculated density of valence states (calculated by a DFT method with the B3LYP/6-31G* basis set on P3HT with ten repeated thiophene ring units; the longer bars indicating that the electronic states include the contribution from S 3p_z atomic orbitals). The left panel shows the spectra of the complete valence region; the right one shows the HOMO spectral region.

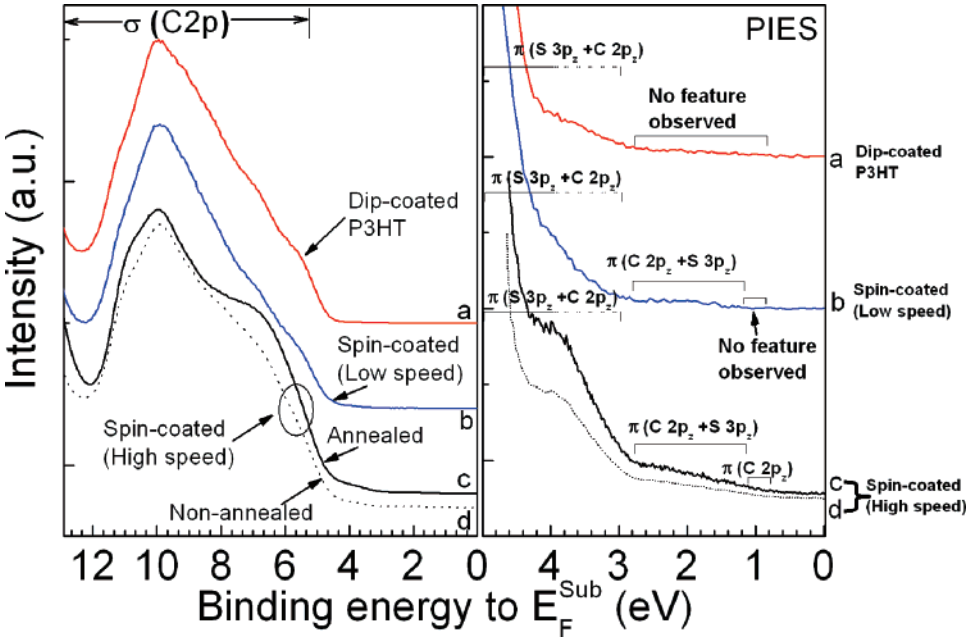

Figure 6. PIES spectra for (a) annealed dip-coated P3HT thin films, (b) annealed low-speed spin-coated, (c) annealed high-speed spin-coated, and (d) nonannealed high-speed spin-coated. The left panel shows the spectra of the complete valence region; the right one shows the HOMO spectral region.

tion at both bulk and surface region. The intensity of σ states related to the hexyl side groups in high-speed spin-coated thin film also is stronger than that in another two samples, which is shown as an obvious shoulder in the range of 6-8 eV in the spectrum, exhibiting that the σ orbitals (i.e., the side hexyl chains) are preferentially oriented parallel to the surface. It is noted that the π electronic structure of high-speed spin-coated P3HT is approximately similar to that of PT in the low binding energy region (0−5 eV). The difference in the higher binding energy region (larger than 5 eV) comes from the effect of the σ electronic states brought by the attached hexyl chains. There is not much difference observed for low-speed spin-coated sample and dip-coated sample in PIES spectra, because the metastable He* atoms can only interact with the electronic states of side hexyl chains extending outside the surface in both samples. The extended side hexyl chains prevent the He* atoms interacting with the polymer main chain and therefore there is no clear feature observed in the low binding energy region (0−3 eV), indicating the electron density contributed from polymer backbone is buried by the side chains.

Comparison of spectra c and d in Figures 5 and 6 shows that the annealed thin films give stronger intensities in the observed features due to the improved crystallinity and ordered structure after annealing, as discussed previously.[18] The π electronic wavefunction from the polymer backbone can be detected by the most surface-sensitive PIES for high-speed spin-coated

P3HT thin films before and after annealing, indicating that the outermost surface layer adopts a similar face-on conformation for these two thin films. Therefore, it assures that annealing-induced increment of molecular tilt angle (α) does not occur in the outermost surface region that differs from the bulk region in the thin films.

3.5. Implication for Device Application. We have demonstrated that the molecular orientation in the surface region of the P3HT thin films and therefore the electron density distributed outside the surface can be controlled by varying the coating parameters. It is evident that the solvent in the bulk can generally keep a longer time than that at surface, which may lead to stronger $\pi-\pi$ stacking domains before the solvent eventually dries off.[15] Conversely, the faster removal of the solvent residual in the surface region than that in the bulk region can quench the process to achieve thermo-dynamic equilibrium structure and result in the surface chain conformation without persisting to the strong bulk orientation preference.[14,15,28] Nevertheless, the solvent removal process can be controlled intentionally to achieve a slower removal rate similar to that in the bulk region, which can give the polymer chains in the surface region time to adopt a more nearly pseudo-equilibrium structure persisting to the bulk orientation preference. Therefore, it is believed that, for low-speed spin-coated and dip-coated thin films, there exists a strong interchain $\pi-\pi$ interaction in the surface layer of the thin films due to the delocalization of π-electrons among the polymer backbones, which gives better ordered surfaces with edge-on conformation and side chains extending outside the surface. However, weaker interchain $\pi-\pi$ interaction of the polymer main chains exists in the surface layer of the thin films coated at high spin speed due to the side chains spacing out the polymer backbones, which results in more disordered surfaces with face-on conformation and polymer backbone exposed outside.

If the He* atoms in PIES technique are considered to be overlayer molecules, the π electron wavefunctions of the overlayer molecules can overlap with the π electronic wavefunctions from the polymer backbone of the sample with face-on conformation. But, otherwise, the overlap between the π electronic wavefunction from the polymer backbone and that from overlayer molecules cannot be expected for polymer thin films with edge-on conformation as directly observed with PIES. Therefore, the implication of $\pi-\pi$ overlap with overlay molecules can be obtained for the heterojunction structure used in the polymer devices when P3HT films are spin-coated at high speed.

The overlap of the π-orbitals within the lamellae in the polymer thin films results in an extended π-system to form an additional intermolecular interaction along which the electrons are delocalized, which has been invoked to be the reason for the high intralayer mobility in P3HT films. Because the side hexyl chains have large badgaps and should act as insulators,[18,29] π-faces normal and the chain backbone are only the directions along which charges transport. The edge-on conformation was said to provide two-dimensional intralamellar charge transport to achieve higher hole mobility and subsequently better $\pi-\pi$ wave function overlap in the source-drain plane for a polymer field effect transistors.[2,13] Thin films with face-on conformation have interchain boundaries terminated with insulating alkyl chains on two sides in lateral directions, effectively blocking lateral charge transfer to neighboring chains in such a transistor. However, in a polymer-based device with layer-by-layer configuration, the face-on conformation of P3HT in the surface region may provide efficient hole transfer to the overlayer molecules due to the possibility of increased $\pi-\pi$ wave function overlap.

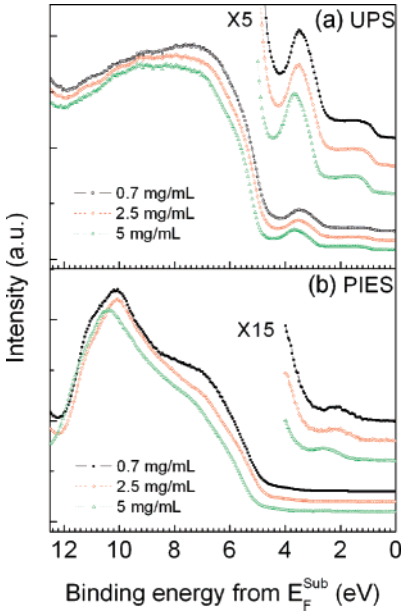

Figure 7. (a) UPS spectra and (b) PIES spectra for annealed P3HT thin films spin-coated at a fixed spin speed (3000 rpm) with various solution concentrations (0.7, 2.5, and 5 mg/mL).

3.6. Solution Concentration Dependence of Surface Electronic Structure of P3HT Thin Films. Surface electronic structures of organic materials are usually very sensitive to the thickness due to the interlayer interaction inside thin films. However, to investigate the thickness dependence on the surface property of solution processed conjugated polymers with an ex situ preparation process is difficult to realize. Cascio and Schlaf et al.[12] has studied the thickness dependency with in situ prepared P3HT thin films by electrospray injection to evaluate the electronic structure of the P3HT/substrate interface. Here, we prepared P3HT thin films with different thickness by spin coating using various solution concentrations (0.7, 2.5, and 5 mg/mL) at a fixed spin speed (3000 rpm). The lower solution concentration is supposed to give thinner films, but the higher solution concentration would provide thicker films. It should be noted that the polymer chain conformation is very much dependent upon the rate of the solidification,[13,15] that is, proportional to the spin speed.[30] Therefore, one may expect that all the films prepared at the fixed speed would have similar polymer chain orientations. The UPS and PIES spectra of these thin films prepared with different solution concentration are shown in Figure 7a,b, respectively. The very similar features independent of the concentration in both the UPS and PIES spectra for these thin films indicate that the polymer chain conformation does not change much for P3HT thin films with different thicknesses. This conclusion is consistent with the NEXAFS results in Table 1 and the previous report by DeLongchamp et al.[13] that the systematic variation of the conjugated plane orientation is related to changes in the solvent evaporation upon the spin speed, but not film thickness. It can be seen, in Figure 7, that the energy position of observed features is shifted slightly to higher binding energy due to the charging effect of the thicker thin films. Further detailed study on this is still in progress in our group.

4. Conclusions

In summary, we have shown that the interchain $\pi-\pi$ interaction and the distribution of the electron density contrib-

uted from the polymer backbone can be intentionally controlled in the surface region of thin films by varying the coating parameters/methods. Surface electronic structures of P3HT thin films with different conformations were investigated by various surface-sensitive spectroscopic techniques (NEXAFS, UPS, and PIES). Especially, the metastable He* atoms in PIES enabled the observation of electronic density distributed outside the polymer surface. The spatial distribution of π electronic states was observed in the range from the inner layer to the outermost surface, which varies with the polymer conformation. Different distributions of π electronic states at the P3HT thin film surface will benefit the charge transfer to a neighboring material for different device configurations by the possibility of increased $\pi-\pi$ electronic wave function overlap.

Acknowledgment. X.T. H. gratefully acknowledges the JSPS fellowship for foreign researchers. We thank Prof. N. Uekawa for XRD measurement. This work was supported partly by a Grant-in-Aid for Creative Scientific Research from JSPS (14GS0213) and the 21st Century COE Program of MEXT (Frontiers of Super-Functionality Organic Devices, Chiba University).

References and Notes

(1) Bernius, M. T.; Inbasekaran, M.; O'Brien, J.; Wu, W. *Adv. Mater.* **2000**, *12*, 1737.
(2) Sirringhaus, H.; Brown, P. J.; Friend, R. H.; Nielsen, M. M.; Bechgarrd, K.; Langeveld-Voss, B. M. W.; Spiering, A. J.; Jassen, R. A. J.; Meijer, E. W.; Herwig, P.; de Leeuw, D. M. *Nature* **1999**, *401*, 685.
(3) Hoppe, H.; Sariciftci, N. S. *J. Mater. Res.* **2004**, *19*, 1924.
(4) Patil, A. O.; Heeger, A. J.; Wudl, F. *Chem. Rev.* **1988**, *88*, 183.
(5) Yang, C. Y.; Soci, C.; Moses, D.; Heeger, A. J. *Synth. Met.* **2005**, *155*, 639.
(6) Derue, G.; Coppée, S.; Gabriele, S.; Surin, M.; Geskin, V.; Monteverde, F.; Leclère, P.; Lazzzroni, R.; Damman, P. *J. Am. Chem. Soc.* **2005**, *127*, 8018.
(7) Salaneck, W. R.; Inganäs, O.; Thémans, B.; Nilsson, J. O.; Sjögren, B.; Österholm, J. E.; Brèdas, J. L.; Svensson, S. *J. Chem. Phys.* **1988**, *89*, 4613.
(8) Sohn, Y.; Richter, J.; Ament, J.; Stukless, J. T. *Appl. Phys. Lett.* **2004**, *84*, 76.
(9) Kim, D. H.; Jang, Y.; Park, Y. D.; Cho, K. *Langmuir* **2005**, *21*, 3203.
(10) Terada, Y.; Choi, B. K.; Heike, S.; Fujimori, M.; Hashizume, T. *Nano Lett.* **2003**, *3*, 528.
(11) Feng, D. Q.; Caruso, A. N.; Schulz, D. L.; Losovyj, Y. B.; Dowben, P. A. *J. Phys. Chem. B* **2005**, *109*, 16382.
(12) Cascio, A. J.; Lyon, J. E.; Beerbom, M. M.; Schlaf, R.; Zhu, Y.; Jenekhe, S. A. *Appl. Phys. Lett.* **2006**, *88*, 062104.
(13) Delongchamp, D. M.; Vogel, B. M.; Jung, Y.; Gurau, M. C.; Richter, C. A.; Kirillov, O. A.; Obrzut, J.; Fisher, D. A.; Sambasivan, S.; Richter, L. J.; Lin, E. K. *Chem. Mater.* **2005**, *17*, 5610.
(14) Kline, R. J.; McGehee, M. D.; Toney, M. F. *Nature Mater.* **2006**, *5*, 222.
(15) Ho, P. K. H.; Chua, L. L.; Dipankar, M.; Gao, X.; Qi, D.; Wee, A. T. S.; Chang, J. F.; Friend, R. H. A*dv. Mater.* **2007**, *19*, 215.
(16) Harada, Y.; Masuda, S.; Ozaki, H. *Chem. Rev.* **1997**, *97*, 1987.
(17) Kera, S.; Abduaini, A.; Aoki, M.; Okudaira, K. K.; Ueno, N.; Harada, Y.; Shirota, Y.; Tsuzuki, T. *Thin Solid Films* **1998**, *278*, 327−329.
(18) Hao, X. T.; Hosokai, T.; Mitsuo, N.; Kera, S.; Mase, K.; Okudaira, K. K.; Ueno, N. *Appl. Phys. Lett.* **2006**, *89*, 182113.
(19) Kera, S.; Setoyama, H.; Kimura, K.; Iwasaki, A.; Okudaira, K. K.; Harada, Y.; Ueno, N. *Surf. Sci.* **2001**, *482-485*, 1192.
(20) Yasufuku, H.; Meguro, K.; Akatsuka, S.; Setoyama, H.; Kera, S.; Azuma, Y.; Okudaira, K. K.; Hasegawa, S.; Harada Y.; Ueno, N. *Jpn. J. Appl. Phys.***2000**, *39*, 1706.
(21) Okudaira, K. K.; Kera, S.; Setoyama, H.; Morikawa, E.; Ueno, N. *J. Electron Spectrosc. Relat. Phenom.* **2001**, *121*, 225.
(22) Becke, A. D. *J. Chem. Phys.* **1993**, *98*, 5648.
(23) Lee, C.; Yang, W.; Parr R. G. *Phys. Rev. B* **1988**, *37*, 785.
(24) Jiang, X. M.; Österbacka, R.; Korovyanko, O.; An, C. P.; Horovitz, B.; Janssen, R. A. J.; Vardeny, J. V. *Adv. Funct. Mater.* **2002**, *12*, 587.
(25) Patnaik, A.; Okudaira, K. K.; Setoyama, H.; Mase, K.; Ueno, N. *J. Chem. Phys.* **2005**, *122*, 154703.
(26) Kera, S.; Yamane, H.; Sakuragi, I.; Okudaira, K. K.; Ueno, N. *Chem. Phys. Lett.* **2002**, *364*, 93.
(27) Yamane, H.; Nagamatsu, S.; Fukagawa, H.; Kera, S.; Friedlein, R.; Okudaira, K. K.; Ueno, N. *Phys. Rev. B* **2005**, *72*, 153412.
(28) Durell, M.; MacDonald, J. E.; Trolley, D.; Wehrum, A.; Jukes, P. C.; Jones, R. A. L.; Walker, C. J.; Brown, S. *Europhys. Lett.* **2002**, *58*, 844.
(29) Duhm, S.; Glowatzki, H.; Rabe, J. P.; Koch, N.; Johnson, R. L. *Appl. Phys. Lett.* **2006**, *88*, 203109.
(30) Meyerhofer, D. *J. Appl. Phys.* **1978**, 3993.